Host factors underlying genetic susceptibility to Xanthomonas infection: a study of a neglected tropical disease in passion fruit (Passiflora alata)

Jéssica Luana Souza Cardoso
Universidade de Sao Paulo Escola Superior de Agricultura Luiz de Queiroz
Zirlane Portugal da Costa
Universidade de Sao Paulo Escola Superior de Agricultura Luiz de Queiroz
Lucas Amoroso Lopes de Carvalho
Universidade Estadual Paulista Julio de Mesquita Filho
Alessandra Alves de Souza
Instituto Agronômico de Campinas: Instituto Agronomico
Daniel Guariz Pinheiro
Universidade Estadual Paulista Julio de Mesquita Filho
Maria Lucia Carneiro Vieira (mlcvieir@usp.br)
Universidade de Sao Paulo Escola Superior de Agricultura Luiz de Queiroz https://orcid.org/0000-0003-0341-5714

Research Article

Keywords: Biotic stress, Xanthomonas axonopodis, Passion fruit, RNA-Seq, De novo transcriptome assembly; Susceptibility genes

Posted Date: May 23rd, 2023

DOI: https://doi.org/10.21203/rs.3.rs-2883157/v1

Abstract

De novo RNA-Seq assembly facilitates the study of transcriptomes of non-model, underutilized crops, enabling researchers to capture the maximum number of genes expressed in plant tissues. We were able to describe the expression profiling of the sweet passion fruit (*Passiflora alata*) in response to *Xanthomonas axonopodis* pv. *passiflorae*(*Xap*) infection. The crop is appreciated for the typical aroma and characteristic flavor of its fruits. However, yield is impaired by *Xap*, whose effects are exacerbated by high temperature and humidity. Initially, we provided the *P. alata* transcriptome assemblies which were shown to have high completeness, based on the expected gene content for a *de novo* transcriptome assembly. A total of 1,329 were completed genes and 96.6% of the orthologs conserved across Embryophytes were represented in the assembled transcriptome. Genes involved in pathogen recognition such as PRRs, *R* genes and genes related to the signaling cascade, coding for specific transcription factors and secondary metabolites, were found to be upregulated after infection. *P. alata* is known to be susceptible to *Xap*, thus we were interested in identifying possible susceptibility (*S*) genes. Interestingly, both characterized *S* genes in other plant species i.e., *SWEET10* and *LOB1*were found to be upregulated in *P. alata*, suggesting that an effector-triggered susceptibility was achieved through the interaction between *Xap* and *P. alata*. Our qPCR results corroborate the role played by these genes, which could potentially be targets for genome editing in order to produce disease-resistant cultivars.

Introduction

The genus *Xanthomonas* consists of some 30 plant-associated species, many of which cause important diseases in food crops and ornamentals, causing yield losses and impacting agriculture and food safety worldwide. The resulting diseases include bacterial blight, canker, bark necrosis, black rot, leaf scald, leaf spot, leaf streak and wilt. Individual species (e.g., *Xanthomonas axonopodis*) comprise multiple pathovars, characterized by distinct host-specificity or mode of infection. Most species and pathovars are widely distributed and well-studied. For instance, complete or draft genome sequences are available for several *Xanthomonas* strains, including vascular and nonvascular plant pathogens (reviewed in Nakayinga et al. 2021).

The plants' defense response has been consensually described as a two-stage process. First, pattern recognition receptors (PRRs) recognize microbe-associated molecular patterns (MAMPs), which are highly conserved molecular signatures. This recognition initiates an initial defense response, called pathogen-triggered immunity (PTI). As a countermeasure, as in the case of *Xanthomonas* spp., the pathogen injects effectors such as transcription activator-like effectors (TALEs) into the host cells via the type III secretion system (T3SS). These effectors boost plasticity in bacterial adaption to host plants. They directly bind to target DNA via a rearrangeable central domain of tandem repeats, e.g., promoters of susceptibility genes rendering the host more vulnerable to infection (see Timilsina et al. 2020; Teper and Wang 2021). *Xanthomonas* spp. effectors can also activate resistance (*R*) genes and produce a second defense response called effector triggered immunity (ETI). Recognition of the pathogen by the host, either through PRRs or *R* genes, triggers a series of mechanisms in an attempt to inhibit pathogen proliferation. The mechanisms involved include an increase in calcium influx, accumulation of reactive oxygen species (ROS), stimulation of a signaling cascade by MAP kinases or calcium-dependent sensor proteins, and activation of transcription factors (TFs) which, in turn, play a part in cellular reprogramming and the production of hormones and antimicrobial compounds (reviewed in Toruño et al. 2016; Timilsina et al. 2020; Cardoso et al. 2022; Aftab and Roychoudhury 2021).

Xanthomonas axonopodis pv. *passiflorae* (*Xap*) causes bacterial spots on leaves and fruits in cultivated *Passiflora* species, popularly known as passion fruits. *Xap* is one of the most important crop pathogens, and it impairs fruit shelf life. The bacterium can live both externally on or internally in the host, penetrating plant cells through natural openings, such as stomata and hydathodes, or through lacerations. Once inside the plant, the bacterium can reach the vascular system and spread throughout the plant's tissues. In leaves, the pathogen induces chlorosis and necrosis, and lesions may coalesce

causing leaf drop or even plant death in severe cases. Spots are also formed on fruits, rendering them unattractive to the consumer (Ishida and Halfeld-Vieira 2009).

There is no effective control against the disease caused by *Xap*, although some induced resistance has been reported (Boro et al. 2011). Preventive measures include the use of disease-free seeds, seed and leaf treatments, and chemical compounds containing copper. However, these approaches are not completely effective and could be harmful to the environment.

The development of disease-resistant cultivars is crucial (Fischer and Rezende 2008) and may include introduction from an outside source, selection of tolerant genotypes, and generation of novel variations via biotechnological intervention. Importantly, we learned in a previous study that *Passiflora edulis* (sour passion fruit) is susceptible and its response to *Xap* is under oligogenic control (Lopes et al. 2006). Nevertheless, no studies have focused on unveiling gene expression levels across the transcriptome. Therefore, we have evaluated the expression profiling of *P. alata* (sweet passion fruit) in response to *Xap* inoculation using RNA-seq technology. Our results provide a complete view of the pathways activated in the plant host under infection. Importantly, we have identified two susceptibility (*S*) genes that were upregulated in response to *Xap*, which could be potential targeted for gene silencing, a fast-moving area of plant research aiming disease control.

Materials and Methods

Bacterial inoculation and RNA isolation

Sweet passion fruit clones from the 'SV3' accession were kept under greenhouse conditions for 150 days. This plant accession (Fig. 1a) is an indoor selection collected from a commercial orchard located in the Southeast region of Brazil (22°17' S, 51°23' W). It is a vigorous plant that was used as a male parent of a segregating population from which promising genotypes were selected to improve fruit quality and yield (Pereira et al. 2017; Chavarría-Perez et al. 2020).

For leaf inoculation, a bacterial suspension of a virulent isolate (AP302) was obtained following the protocol described in Munhoz et al. (2011). The virulence of this isolate was previously evaluated in a collection of ~90 *Xap* isolates kept in our laboratory. The progression of lesions on the leaves after inoculation with *Xap* is shown in Fig. 1. In brief, to prepare the inoculum, the AP302 isolate was grown in liquid nutrient medium for 24 hours at 28ºC and 150 rpm. Then, 100 µL of the bacterial suspension was plated on nutrient agar medium and the plates incubated (24 h, 28ºC). After growth of the culture, 20 mL of a saline solution (NaCl 0.85%) were added to suspend the colonies. The suspension was then homogenized and standardized in a spectrophotometer to an optical density of 0.3 at 600 nm, which corresponds to an approximate bacterial concentration of 10^8 CFU/mL.

A total of six biological replicates of each treatment (inoculated and control) were established. To do this, rooted cuttings from the 'SV3' accession were grown in plastic pots until fully developed. At first, bacterial cells were dispersed at the edges of punched leaf holes (0.5 cm in diameter) using a cotton swab previously moistened with bacterial cells. The leaves of the controls were mock inoculated with 0.85% NaCl solution. Leaves were collected 5 days after inoculation (DAI). In order to confirm the efficiency of the inoculation procedure, all inoculated and mock-inoculated plants were kept for disease symptom evaluation at one month after inoculation (Fig. 1).

Immediately after harvesting the leaves, fragments of approximately 4 cm^2 were excised to include the entire bacterial dispersal area. These fragments were frozen and macerated in liquid nitrogen, then stored at −80°C pending total RNA extraction. TRIzol reagent (Invitrogen, USA) was used following manufacturer's instructions. The concentration of total RNA was determined by Qubit™ RNA BR Assay (Thermo Fisher Scientific, USA), and the RNA integrity value (RIN) checked in an RNA 6000 Pico LabChip of Agilent 2100 Bioanalyzer (Agilent, USA).

Library preparation and RNA sequencing

Six sequencing libraries were generated using the TruSeq Stranded mRNA Library Prep Kit (Illumina, USA), according to the manufacturer's instructions. Library preparation is a required sequencing step and involves the introduction of short adapter sequences at the ends of the cDNA templates. Sequencing was then performed on Illumina's NextSeq 2000 platform using the paired end strategy (2×100 bp), generating 50 million reads (Supplementary Fig. S1).

Bioinformatic analysis

First, the FastQC computational program (Andrews 2010) was used to check the quality of the raw sequence data. This procedure was repeated after the processing step. Then, Atropos v.1.1.24 (Didion et al. 2017) was used for removing remnants of adapter sequences from both read ends. Low-quality sequences (average Q-score less than 20), poly-A tail remnants (minimum of 5 consecutive bases at the 5' end), low-complexity readings (DUST score above 30) and those that did not have a minimum length of 20 bases were all eliminated by the PRINSEQ program (Schmieder and Edwards 2011).

Once the reads were checked for quality and processed, and because there is no reference genome for *P. alata* available, a *de novo* assembly was performed with default parameters on Trinity v.2.11.0 (Grabherr et al. 2011). The aim of *de novo* transcriptome assembly is to accurately reconstruct the complete set of transcripts that are represented in the read data, in the absence of a reference genome. Therefore, to evaluate the completeness and accuracy of the *de novo* assemblies, BUSCO v.5.4.3 with the Embryophytes ortholog database (Manni et al. 2021) and TransRate v.1.0.3 (Smith-Unna et al. 2016) analysis were run, respectively, with default settings.

Next, protein-coding regions were predicted from the transcriptome reference assembly using TransDecoder v.5.5.0 (Haas et al. 2013), and then subjected to further functional annotation based on pre-computed ortholog assignments from the eggNOG database using EggNOG-mapper v.2 (Huerta-Cepas et al. 2017).

We assessed changes in gene expression by comparing the data from mock-inoculated (controls) and inoculated leaves using DESeq2 v.1.37.6 (Love et al. 2014). The first step in the differential expression analysis workflow is read-count normalization, which is necessary to make accurate comparisons between samples. First, for each gene, DESeq2 uses the geometric mean across all samples. For every gene, the ratios (sample/geometric mean) are calculated. The median value of all ratios for a given sample is taken as the normalization factor for that sample. Then, the normalized count values are computed using the normalization factor. This is done by dividing each raw count value in each sample by that sample's normalization factor to generate normalized count values. Finally, the relative expression is calculated. In summary, counts are normalized using DESeq2 and differentially expressed genes were filtered using a false discovery rate (FDR) < 0.05 and a Log_2 (fold change) > 1.5 and < −1.5 for biological significance.

To identify which transcript functions and pathways were the most represented, GO functional enrichment analysis was carried out on GOATOOLs software v.1.2.3 (Klopfenstein et al. 2018), with FDR ≤ 0.05 to obtain GO annotations on the "biological process" (BP), "molecular function" (MF) and "cellular component" (CC) categories.

Real Time quantitative PCR (RT-qPCR)

The expression of some genes, selected on the basis of their biological function, was confirmed through RT-qPCR at 5 and 7 DAI. Total RNA was extracted as described above and quantified using the Qubit™ RNA BR Assay (Thermo Fisher Scientific, USA), and 1 µg of RNA was used for cDNA synthesis using the GoScript Reverse Transcription System (Promega, USA).

Gene-specific primers were designed using Primer3web v.4.1.0 (Supplementary Table S1). Two housekeeping genes, *GAPDH* (glyceraldehyde-3-phosphate dehydrogenase) and *ß-Actin,* were used as internal references (Yu et al. 2019). These

genes have been routinely used for the normalization of data in RT-qPCR experiments, and their mRNA expressions remained stable in mock-inoculated and inoculated leaves of *P. alata*.

Amplifications were carried out in a 48-well reaction plate using the StepOne Plus PCR system (Applied Biosystem, USA) and the Power up SYBR™ Green PCR Master Mix (Applied Biosystems, USA). PCR cycling consisted of one denaturation step at 95 °C for 10 min, followed by 40 cycles of 95 °C for 15 s and 60 °C for 1 min, plus a melting curve. This melting curve pattern was used for verifying the specificity of the amplification product and the possible presence of primer dimers.

The amplification efficiency of each pair of primers was determined by generating a standard 5-point curve, based on serial dilutions of cDNA samples. Efficiency was calculated from the slope of the generated standard curve based on the equation E=10(−1/slope). Typically, desired amplification efficiencies range from 90% to 110% (Rutledge and Côté 2003). The relative expression levels of the selected genes by RT-qPCR were calculated using the 2-ΔΔCT method (Livak and Schmittgen 2001). RT-qPCR was performed using 3 biological replicates. Each of these biological replicates was run in 3 technical replicates. The Pearson correlation coefficient (*r*) was used to assess the association between RNA-seq and RT-qPCR fold change values obtained for 4 differentially expressed genes at 5 DAI.

Characterization of *SWEET10* and *LOB1* genes in *Passiflora*

The lack of a high-quality and well-annotated *Passiflora* reference genome inspired our group to assembling a draft genome of *P. organensis*, a wild species with a small genome size of ~260 Mb (Costa et al. 2021). The genome annotation is available at https://genomevolution.org/coge/GenomeInfo.pl?gid=59125 and was used in a blast search to find the *SWEET10* and *LOB1* genes. The search was run on tblastx, using the transcripts of *P. alata* found in the present study as queries, an e-value of 1e-5 and the BLOSUM62 matrix. For domain characterization, all fasta sequences were subjected to CDD blast (Lu et al. 2020) using default parameters. To predict the transmembrane domains of *SWEET10* genes, the CCTOP (Consensus Constrained TOPology, Dobson et al. 2015) and Protter (Omasits et al. 2014) web servers were used with default parameters.

Results

Sequencing and *de novo* assembly

Approximately 300 million raw reads were generated from 6 RNA libraries, an average of 50 million (2× 100 bp) per library (PRJNA898380). After processing, a total of 323.737.390 clean reads (111 Gb of clean data) were retained. Quality checking with FASTQC indicated that our data were of high quality, since a quality score of at least Q30 was achieved, meaning that 100% of the reads were perfect, with no errors or ambiguities.

The reads were then *de novo* assembled into 132,698 contigs. The mean contig length was 1,493 bp, and the minimum contig length to cover 50% of the assembled transcriptome (N50) was 2,498 bp. Most (95%) of the fragments were mapped and only 0.04% were uncovered. The GC content was 42%, similar to the value published for the genomes of *Passiflora edulis* (38.7%; Xia et al. 2021) and *Passiflora organensis* (38.3%; Costa et al. 2021). The TransRate assembly score was 0.4187; this score ranges between 0 and 1.0 and is calculated using the geometric mean of all contig scores multiplied by the proportion of input reads that support the assembly. All these metrics (see Table 1) were delivered by TransRate, software specifically designed to provide insight into the accuracy and completeness of any *de novo* assembled transcriptome (Smith-Unna et al. 2016).

BUSCO assessment of the quality of *P. alata* transcriptome assemblies revealed high completeness, based on the expected gene content for a *de novo* transcriptome assembly. A total of 1,329 were completed genes, 477 single-copy genes and 852 duplicated genes. In other words, 96.65% of the orthologs conserved across Embryophytes were represented in the

assembled transcriptome, which exhibited low fragmentation (2.32%) and few missing sequences (1.02%) (Supplementary Fig. S2).

Table 1
Statistics for the *Passiflora alata de novo* transcriptome based on TransRate assembly scores

Parameter	Result
No. Sequences (contigs)	132,698
Smallest contig (bp)	194
Largest contig (bp)	2,2344
Bases	198,217,177
Mean length (bp)	1,493.74
Contig N50 length (bp)	2,498
% Guanine-Cytosine content	42
Fragments	172,501,242
Fragments mapped	163,069,356
% Fragments mapped	94.50
Good mappings	139,689,627
% Good mappings	80.90
Bad mappings	23,379,729
Bases uncovered	18,434,500
% Bases uncovered	9.59
Contigs uncovered	4,755
% Contigs uncovered	3.58
Contigs segmented	12,252
% Contigs segmented	9.23
TransRate assembly score	0.4187
Good contigs	128,711
% Good contigs	9.69

Differential gene expression analysis

A total of 1,242 transcripts were identified as differentially expressed, considering that both *p*-value (< 0.05) and Log_2 (fold-change) criteria were simultaneously satisfied. These included 604 downregulated and 638 upregulated in the inoculated group compared to the control group. The top 100 transcripts downregulated and upregulated are listed in the Supplementary Table S2 and Supplementary Table S3, respectively.

A volcano plot was used to display RNA-seq results (Fig. 2) and to facilitate visual identification of genes with large fold changes (x-axis) that are also statistically significant (y-axis). In the plot, the most downregulated genes are towards the

left (in blue) and the most upregulated genes towards the right (in red); the most statistically significant genes are towards the top.

Coding region identification and functional enrichment analyses

As mentioned above, a *de novo* assembly approach involves reconstructing a novel transcriptome from organisms with no referenced genome available for alignment. Newly assembled transcripts encode proteins whose homology with known proteins cannot always be detected. Therefore, the TransDecoder tool was used to capture sequence-coding regions, as it predicts coding regions based on metrics tied to sequence composition (Haas et al. 2013). We first selected the best single open reading frame (ORF) per transcript. Importantly, 75% of them are classified as “complete ORFs”, found to contain the first and the stop codons (Supplementary Fig. S3).

In addition, an enrichment analysis was performed based on Gene Ontology (GO) terms. The transcripts differentially expressed (inoculated and mock-inoculated groups) were assigned to three categories: cellular component, molecular function, and biological process. To do this, we extracted the top 10 GO terms in each category that were up- (Fig. 3a) or downregulated (Fig. 3b). Briefly, in both cases, the most enriched terms in the “Biological Processes” category were cellular (0009987) and metabolic (GO:0008152) processes, response to stimuli (GO:0050896) and biological regulation (GO:0065007). In the “Cellular Component” category, the cellular anatomical entity (GO:0110165), organelle (GO:0043229) and membrane (GO:0016020) stand out. Finally, in the category “Molecular function”, the most enriched terms are catalytic (GO:0003824) and hydrolytic activity (GO:0016787), binding (GO:0005488) and transcription regulator activity (GO:0140110) (Fig. 3).

Gene expression profiling of passion fruit in response to bacterial infection

Analysis of host transcript levels revealed genes differentially activated in response to infection (Table 2). The expression of several genes associated to defense mechanisms was significantly modulated, and a hypothetical model using heatmaps and literature information is proposed to explain the *P. alata* defense strategy (Fig. 4).

It seems that the host recognizes pathogen/microbe-associated molecular patterns (PAMPs/MAMPs) through PRRs since seven PRRs were found to be upregulated (FDR < 0.5, $-1.5 < \text{Log}_2 > 1.5$), all belonging to the large family of receptor-like kinases (RLKs) (Fig. 4; Table 2. These genes included three with a leucine-rich repeat (LRR) ligand-binding ectodomain which functions to identify plant- and pathogen-derived peptide epitopes; three with a G-Lectin ectodomain that recognizes lipopolysaccharide (LPS); and one with a lysin ectodomain, which is involved in the recognition of pathogenic peptidoglycan (PGN). The expression of BAK1 (BRASSINOSTEROID INSENSITIVE 1-associated receptor kinase 1) gene was also induced and it is generally recruited to form a major phosphorylation complex between the kinase domains of the RLKs in order to trigger a PTI signaling cascade (Kemmerling and Nürnberger 2008), reinforcing the hypothesis of PRR-*Xap* recognition.

In addition, a possible increase in calcium influx and accumulation of ROS is suggested by the upregulation of a gene (RBOHD) that codes for a respiratory burst oxidase homolog protein D and is a calcium-dependent NADPH oxidase (Kadota et al. 2014). Thus, a signaling cascade seems to be activated mediated by hormone signaling, resulting in the activation of TFs that regulate the expression of target genes. Nine and 12 genes respectively associated with hormone signaling and TFs were identified (Table 2). Genes involved in the hormonal pathway of salicylic acid (SA), ethylene and auxin were upregulated. Among the TFs, the WRKY family was the most abundant (Fig. 4; Table 2). The downstream upregulated defense mechanism included the induction of three pathogenesis-related (PR) genes, two genes encoding antimicrobial compounds, and two cell wall related genes.

Interestingly, besides a typical PTI response, the expression of two *R* genes associated with ETI was induced (Fig. 4; Table 2), one with a TIR (toll interleukin receptor) domain and the other with a CC (coiled-coil) domain. In addition, two *S*

genes of *P. alata* were found to be upregulated after infection (*SWEET10* and *LOB1*), lending weight to the idea that these genes lead to host susceptibility in this compatible interaction. *Xanthomonas* spp. effectors are known to be able to bind to host *S* genes, impairing resistance (Teper et al. 2020).

Our results confirm that *P. alata* is a susceptible host, similarly to the response of *P. edulis* to *Xap* (Munhoz et al. 2015). Thus, *Xap* might secrete effectors that suppress ETI, leading to a ETS response, activating *SWEET10* and *LOB1* by TALE effectors, to facilitate bacterial colonization in both host environment. If so, we expected that such *R* genes be repressed in later stage of infection. To test this hypothesis, the expression levels of *R* and *S* genes were also evaluated at 7 DAI, when the first disease symptoms are observed. Indeed, no induction of *R* genes occurred in later stage of infection, but induction of *S* genes remained (Fig. 5). Taking together the results indicate that *P. alata* is able to activate PTI and possibly ETI after *Xap* infection, however *Xap* is able to suppress PTI/ETI triggering ETS leading to host susceptibility.

It seems to be a consensus that RNA-sequencing results and the approaches used for data analysis are robust enough and do not always require validation (Coenye 2021). Herein, we demonstrate that RT-qPCR and RNA-seq fold change values are highly correlated (Pearson correlation = 0.83) (Supplementary Fig. S4), thus validating the sequencing results.

Table 2

Selected genes whose expression was significantly altered after the infection of *Passiflora alata* leaves with *Xanthomonas axonopodis*. Positive log_2 values denote genes that have been activated and negative log_2 values those that have been repressed

Code	Gene	Function	Log_2 (fold change)	*p*-value
BAK1	BRASSINOSTEROID INSENSITIVE 1-associated receptor kinase 1-like	PRR	1.19995372377009	0.000423430476913283
Lys-RLK	LysM domain receptor-like kinase 3	PRR	0.839374533524309	0.000273669992871701
G-Lec	G-type lectin S-receptor-like serine/threonine-protein kinase	PRR	7.12290804534244	2.38923365929004e-07
G-Lec/CES1	G-type lectin S-receptor-like serine/threonine-protein kinase CES101	PRR	6.9453742200366	1.26302507796739e-05
G-Lec/RKS1	G-type lectin S-receptor-like serine/threonine-protein kinase RKS1	PRR	6.38212426498823	4.09592564723631e-05
LRR/RFK1	LRR receptor-like serine/threonine-protein kinase RFK1	PRR	0.6521683546703	0.00042586001209681
LRR/RLK	Leucine-rich repeat receptor-like kinase	PRR	2.83055636018882	1.07977574537314e-08
LRR/RLK	Leucine-rich repeat receptor-like kinase	PRR	-6.20967814756505	1.78551079307389e-05
LRR/RLK	Leucine-rich repeat receptor-like kinase	PRR	-0.621078221763 58	0.000502531925238616
PBL28-LRR	LRR receptor-like serine/threonine-protein kinase PBL28	PRR	7.58202619389946	1.64996445522062e-08
RPV1/TIR-NB-LRR	Toll Interleukin1 receptor-nucleotide binding site-leucine-rich repeat	*R* gene	1.02740967492438	0.027863378153449
LR1O/CC-NBS-LRR	Coiled-coil-nucleotide-binding site-leucine-rich repeat LR10	*R* gene	5.43308889724399	0.02558048693673
SWEET10	Sugar efflux transporter SWEET10	*S* gene	8.03551945164662	1.46137767410355e-06
LOB1	Lateral organ boundaries (LOB) gene	*S* gene	1.59357620897032	0.00270069072529042
RBOHD	Respiratory burst oxidase homolog protein D	Signaling	0.828425088653322	2.6120820995625e-05
EP3/Endochitinase	Endochitinase	Pathogenesis-related gene	1.68730735243121	0.0003261682945954
Peroxidase	Belongs to the peroxidase family	Pathogenesis-related gene	5.96975251917162	2.939721786438 61e-0

Code	Gene	Function	Log_2 (fold change)	*p*-value
Glucanase	1,4-beta-D-glucanase-like	Pathogenesis-related gene	2.06486136347498	4.04809404242022e-06
GermacreneD	(-)-germacrene D synthase-like	Antimicrobial compounds	11.6971145381479	5.88742139225596e-23
Nerolidol	(3S,6E)-nerolidol synthase	Antimicrobial compounds	4.87296433161147	0.00015575810686717
Expansin	Expansin-like B1	Cell wall reinforcement	8.2297457242818	2.6634995222482e-10
CSLE6	Cellulose synthase-like protein E6	Cell wall reinforcement	12.1684983977643	4.42486941374679e-20
WAT1	Walls are thin 1	Hormone signaling	5,44319055	0,000251948818908193
SAMT	Salicylate carboxymethyltransferase	Hormone signaling	5.04249148603076	4.16345324023472e-05
EIN4	Protein EIN4	Hormone signaling	0.923502980388925	0.000453212192649248
ERF113	Ethylene-responsive transcription factor ERF113	Transcription Factor	0.83251159914744	0.000263887232933124
ERF109	Ethylene-responsive transcription factor ERF109-like	Transcription Factor	3.90707650523884	0.000186100491803284
ERF.1	Ethylene-responsive transcription factor	Transcription Factor	3.56749368017761	5.20498460921529e-15
ERF.2	Ethylene-responsive transcription factor	Transcription Factor	1.81811834756859	0.000114971935429913
ARF10	Auxin response factors (ARFs)	Hormone signaling	7.21129646559514	2.79134770694059e-06
GH3.1	Indole-3-Acetic acid-amido synthetase GH3.1	Hormone signaling	4.15604106975368	1.43991432886329e-06
WRKY40	WRKY40 Transcription Factor	Transcription factor	4.45834755558982	5.96381881202165e-05
WRKY75	WRKY75 Transcription Factor	Transcription factor	1.94290496560596	1.21396391516257e-05
WRKY33	WRKY33 Transcription Factor	Transcription factor	0.898043991622992	1.86739033510323e-06
WRKY34	WRKY34 Transcription Factor	Transcription factor	-6.06461381583862	0.000187259690617813
WRKY	WRKY Transcription Factor	Transcription factor	-8.8528197504692	0.000491720587509096
WRKY	WRKY Transcription Factor	Transcription factor	-8.63172863690538	8.19943668118033e-08
bHLH35	Transcription factor bHLH35	Transcription factor	10.0226002350337	1.65022140641892e-15

Code	Gene	Function	Log_2 (fold change)	*p*-value
bHLH18	Transcription factor bHLH18	Transcription factor	4.6927641654451	5.98313525333968e-08
MYB.1	MYB family transcription factor APL	Transcription factor	6.83741771221823	1.32165233226577e-06
MYB.2	MYB family transcription factor	Transcription factor	-6.50387926238602	2.93256272995849e-06
RF2b	transcription factor RF2b-like	Transcription factor	6.86358173718873	4.73408673179809e-06
MADS-box23	MADS-box transcription factor 23-like	Transcription factor	10.5877166438556	1.65692964371977e-17
NAP	NAC transcription factor	Transcription factor	3.79916741764454	2.69404498381501e-06
GATA	GATA transcription factor	Transcription factor	2.43745547948583	9.60848479673283e-06
GATA	GATA transcription factor	Transcription factor	8.33678597808368	6.41672338103898e-10
GATA26	GATA transcription factor 26-like	Transcription factor	8.05738924378241	6.16142095504508e-10
GTE4	Transcription factor GTE4	Transcription factor	11.1175265989332	2.1610198141825e-18

Characterization of SWEET10 and LOB1 genes in Passiflora

SWEET are well-known *S* gene that occur in many hosts (see Breia et al. 2021), therefore we decided to characterize them in *Passiflora*. *SWEET* genes encode a protein that functions as a sugar transporter and facilitate the diffusion of sugars across cell membranes (Braun 2012; Slewinski 2011; Chen 2013). Pathogens often use these host transporters because of their source of sugar nutrition. Hence, mutations that block this mechanism have been found to confer pathogen resistance (Gupta 2020; Chen 2013). According to the NCBI Conserved Domain Database (CDD), some members of the PQ-loop superfamily (https://www.ncbi.nlm.nih.gov/Structure/cdd/cl21610) are membrane bound proteins with a pair of repeats each spanning two transmembrane (TM) helices connected by a loop. This superfamily contains five subfamilies: PQ-loop (PFAM04193), CTNS (SMART00679), SWEET (COG4095), MtN3_slv (PFAM03083) and SemiSWEET_2 (NF037968) (Lu et al. 2020). *SWEET* genes belongs to the MtN3_slv subfamily and are known to have 7 TM domains (Xuan et al. 2013).

This is the first study of *SWEET* genes in *Passiflora*. The genome of *P. organensis* has 18 genes that belong to the PQ-loop superfamily. Thirteen of them have the MtN3_slv domain and 10 have 7 TM domains (Fig. 6). The length of *SWEET10* copies ranged from 564 to 1,116 bp (Supplementary File 01). Some *SWEET10* gene copies are located on the same scaffold, possibly due to duplication events (Supplementary Fig. S5).

LOB (*LATERAL ORGAN BOUNDARIES*) genes are involved in many functional processes. Their role as regulators of plant organ development is the most studied. However, recent studies have revealed the functional diversity of *LOB* genes, showing their role in pollen development, plant regeneration, photomorphogenesis and the pathogen response (Xu et al. 2016). Some studies have demonstrated that *LOBs* act as key susceptibility genes, whose expression is activated by *Xanthomonas* spp. Importantly, by editing of the *LOB1* promoter via CRISPR/Cas9 canker-resistant grapefruit (Jia et al. 2022) and sweet orange. (Huang et al. 2022) were generated.

The genome of *P. organensis* has 39 copies of the *LOB1* gene. The length of *LOB1* copies ranged from 441 to 957 bp and all have the characteristic LOB domain (Supplementary Fig. S6). Some *LOB1* gene copies are located on the same scaffold, possibly due to duplication events.

Discussion

Plants have evolved a sophisticated immunity system to detect and try to stop pathogen proliferation and disease progression. We therefore aimed to reveal how the sweet passion fruit responds to infection by *Xap*. This bacterium is reported to be the most serious bacterial disease in orchards, but studies regarding plant-pathogen interaction is still unexplored. Thus, we used RNA-Seq data and a computational workflow of bioinformatics analysis to unveil the genetic mechanism involved in such interaction.

Several approaches are available to assess the quality of transcriptome assemblies, including N50 values, transcript length, and reads mapped back to the transcriptome (RMBT), TransRate, BUSCO, etc. (Sheikh-Assadi et al. 2022). The sequence data were of high quality, as was the *de novo* assembly of the *P. alata* transcriptome, with high contiguity and accuracy. The scores for *P. alata* (= 0.42) were higher than those for *Vigna angularis* (= 0.26), *Hevea brasiliensis* (= 0.16) and *Nicotiana tabacum* (= 0.30). Moreover, the percentage of read mapping herein was high (= 95%), close, for instance, to that of *N. tabacum* (= 93%) and higher than that of *V. angularis* (= 88%) and *H. brasiliensis* (= 89%) (MacManes 2018).

A comparison of BUSCO metrics showed that the majority were of high quality, with 96.6% of embryophyte genes complete and present in the *de novo* assembled *P. alata* transcriptome. Only a small fraction was missing (1.02%) or fragmented (2.32%). In like manner, an assembly of the banana transcriptome in response to *Xanthomonas* infection, but using its genome as a reference, also revealed ~ 96% of complete genes (Tripathi et al. 2019). The BUSCO metrics assess transcriptome assembly and annotation completeness with single-copy orthologs. When applied to the above-mentioned transcriptomes, it was shown that 95% of the genes were complete in *Vigna angularis*, 93.8% in *Hevea brasiliensis* and 95.4% in *Nicotiana tabacum de novo* assemblies.

At the beginning of the infection process, the innate immune system constitutes the first line of defense against invading pathogens and relies on a large family of specific PRRs, which detect distinct evolutionarily conserved structures on pathogens, called PAMPs. This strategy was identified in response to *Xap* in the sweet passion fruit. In our analysis, 7 PRRs with different domains were identified as containing the leucine-rich repeat (LRR), the most predominant, triggering a defense response in different ways. In rice, for instance, LRR receptors Xa3 and Xa26 are related to the induction of autophagy-like cell death, activation of calcium signaling and ROS production (Cao et al. 2019), whereas Xa21 triggers a defense response after recognizing a peptide secreted by *Xanthomonas*, called tyrosine-sulfated type 1 (RaxX), capable of mimicking plant hormones to regulate host responses (Pruitt et al. 2015).

In addition to LRR-PRRs, receptors with the lysin and lectin motif domains have also been identified in *P. alata*, and also in *Citrus sinensis* (Li et al. 2021) and kumquat plants (Giraldo-González et al. 2021), in which 6 and 20 lysin receptors respectively were upregulated under infection with *X. citri* subsp. *citri*. Lysin receptors (Liu et al. 2012) and lectin receptors (Cheng et al. 2013) were found to be upregulated in rice in response to *X. oryzae* pv. *oryzae* (*Xoo*).

The process from pathogen perception to activation of a defense response has been intensively reviewed (Delplace et al. 2022). After pathogen recognition by receptors, a defense response is triggered, and as a counterattack the bacterium secretes effectors inside the host cell. These effectors can be recognized by cytoplasmic receptors encoded by *R* genes, and triggering a new defense response. *R* genes were found to be upregulated in *P. alata*., but not expressed in later stage of infection, suggestion that the pathogen blocked ETI by unknown effectors.

In *Xanthomonas* spp. TALE effectors are known to bind to promoter regions and activate *S* genes. This seems to be the case of *Xap* for modulating *P. alata* genome in its favor, once two *S* genes (*SWEET10* and *LOB1*) were upregulated in

different stages of pathogen colonization (Fig. 4; Fig. 5). These genes may contribute to pathogen proliferation and colonization as observed in other susceptible hosts such as walnut (Jiang et al. 2020) and rice (Eom et al. 2019) in the case of *SWEET10* and *Citrus*, in the case of *LOB1* (Peng et al. 2017).

The *SWEET10* gene (the transcript is 3,054 b in length, NCBI Gene ID: 100817002) encodes sugar transporters and is used by pathogens to provide sugar as a source of nutrition, resulting in successful infection (Gupta et al. 2021). *SWEET10* has also been found to be upregulated under *Xanthomonas* infection and activated by the corresponding TAL effectors, Avrb6 and TAL20, in cassava (Cohn et al. 2014) and cotton (Cox et al. 2017). Silencing *SWEET10* reduced disease symptoms in cotton, corroborating the idea that this gene is required for susceptibility, as reported in walnut (Jiang et al. 2020) and rice (Blanvillain-Baufumé et al. 2017; Eom et al. 2019).

The second *S* gene was *LOB1* (the transcript has 1,062 b, NCBI Gene ID: 778395), which belongs to a plant specific-TF family, characterized by a highly conserved LOB domain. Expansin is directly targeted by *LOB1*. The expansin itself disrupts noncovalent interactions between cellulose microfibrils and matrix polysaccharides, contributing to cell wall loosening and textural changes (Samalova et al. 2022). Expansin and cellulose synthase coding genes were found to be upregulated in inoculated leaves of *P. alata*. In *Citrus*, *LOB1* expression induces pustule formation and activates genes related to cellular expansion. Pustule formation in the infected tissues plays a vital role in canker development and pathogen spread (Hu et al. 2014; Xu et al. 2016). Importantly, through gene editing, *LOB1* knockout boosted *Citrus* resistance, with no canker formation (Peng et al. 2017).

SWEET10 and *LOB1* are important *S* genes in different hosts, but quite surprisingly both were induced in *P. alata–Xap* interaction, suggesting that specific *S* genes could display different function associated with pathogen colonization. Clarifying, *Xap* has an external life, such as *X. citri* subsp. *citri*, which is able to induce the expression of the canker susceptibility gene *LOB1* through a transcription activator-like (TAL) effector (Teper et al. 2020), but a systemic lifestyle such as *X. oryzae* pv. *oryzae*, which also secretes a TAL effector that targets a rice *SWEET* gene (Breia et al. 2021). Taken together, *SWEET* and *LOB* are both recognized susceptibility genes involved in the interaction with *Xanthomonas*. Importantly, this pathosystem remains severely understudied and there is no genome available for *X. axonopodis* pv. *passiflorae*. We believe that our manuscript contributes to unveiling the mechanism that leads to passion fruit susceptibility, opening up new avenues for manipulating these genes for agricultural purposes, rendering plants resistant to pathogen attack. Evidently, future functional studies will be necessary to elucidate the role played by *Xanthomonas* effectors in inducing the expression of passion fruit susceptibility genes and causing disease.

Declarations

Funding

The authors acknowledge the following Brazilian funding agencies: Fundação de Amparo à Pesquisa do Estado de São Paulo (FAPESP, grant no. 2019/07838-6), Coordenação de Aperfeiçoamento de Pessoal de Ensino Superior (CAPES, Finance Code 001) and Conselho Nacional de Desenvolvimento Científico (CNPq).

Competing interests

The authors have no relevant financial or non-financial interests to disclose.

Author Contribution Statement

JLSC planned and prepared all laboratory experiments and drafted the manuscript; ZPC worked for searching and characterizing the susceptibility genes in *Passiflora* genome; JLSC and LALC performed the bioinformatics analysis under the supervision of DGP; AAS revised the manuscript critically for important intellectual content; MLCV conceived the study, contributed to research design, and wrote the final version of the manuscript.

Data Availability

The datasets generated during the current study are available within the article and supplementary materials, and in the NCBI repository.

References

1. Aftab T, Roychoudhury A (2021) Crosstalk among plant growth regulators and signaling molecules during biotic and abiotic stresses: molecular responses and signaling pathways. Plant Cell Rep 40:2017–2019
2. Andrews S (2010) FastQC: a quality control tool for high throughput sequence data
3. Blanvillain-Baufumé S, Reschke M, Solé M, Auguy F, Doucoure H, Szurek B et al (2017) Targeted promoter editing for rice resistance to *Xanthomonas oryzae* pv. *oryzae* reveals differential activities for SWEET14-inducing TAL effectors. Plant Biotechnol J 15:306–317
4. Boro MC, Beriam LOS, Guzzo SD (2011) Induced resistance against *Xanthomonas axonopodis* pv. *passiflorae* in passion fruit plants. Trop Plant Pathol 36:74–80
5. Braun DM (2012) Sweet! The pathway is complete. Science 335(6065):173–174
6. Breia R, Conde A, Badim H, Fortes AM, Gerós H, Granell A (2021) Plant SWEETs: from sugar transport to plant-pathogen interaction and more unexpected physiological roles. Plant Physiol 186:836–852
7. Cao J, Zhang M, Zhu M, He L, Xiao J, Li X et al (2019) Autophagy-like cell death regulates hydrogen peroxide and calcium ion distribution in Xa3/Xa26-mediated resistance to Xanthomonas oryzae pv. oryzae. Int J Mol Sci 21:194
8. Cardoso JLS, Souza AA, Vieira MLC (2022) Molecular basis for host responses to *Xanthomonas* infection. Planta 256(4):84
9. Chavarría-Perez LM, Giordani W, Dias KOG, Costa ZP, Ribeiro CAM, Benedetti AR et al (2020) Improving yield and fruit quality traits in sweet passion fruit: evidence for genotype by environment interaction and selection of promising genotypes. PLoS ONE 15:e0232818
10. Chen L-Q (2013) SWEET sugar transporters for phloem transport and pathogen nutrition. New Phytol 201:1150–1155
11. Cheng X, Wu Y, Guo J, Du B, Chen R, Zhu L et al (2013) A rice lectin receptor-like kinase that is involved in innate immune responses also contributes to seed germination. Plant J 76:687–698
12. Coenye T (2021) Do results obtained with RNA-sequencing require independent verification? Biofilm 3:100043
13. Cohn M, Bart RS, Shybut M, Dahlbeck D, Gomez M, Morbitzer R et al (2014) *Xanthomonas axonopodis* virulence is promoted by a transcription activator-like effector–mediated induction of a SWEET sugar transporter in cassava. Mol Plant-Microbe Interact 27:1186–1198
14. Costa ZP, Varani AM, Cauz-Santos LA, Sader MA, Giopatto HA, Zirpoli B et al (2021) A genome sequence resource for the genus *Passiflora*, the genome of the wild diploid species *Passiflora organensis*. Plant Genome 14(3):e20117
15. Cox KL, Meng F, Wilkins KE, Li F, Wang P, Booher NJ et al (2017) TAL effector driven induction of a SWEET gene confers susceptibility to bacterial blight of cotton. Nat Commun 8:1–14
16. Delplace F, Huard-Chauveau C, Berthomé R, Roby D (2022) Network organization of the plant immune system: from pathogen perception to robust defense induction. Plant J 109:447–470
17. Didion JP, Martin M, Collins FS (2017) Atropos: specific, sensitive, and speedy trimming of sequencing reads. PeerJ. 2017:e3720
18. Dobson L, Reményi I, Tusnády GE (2015) CCTOP: a Consensus Constrained TOPology prediction web server. Nucleic Acids Res 43:W408–W412
19. Eom J-S, Luo D, Atienza-Grande G, Yang J, Ji C, Luu V et al (2019) Diagnostic kit for rice blight resistance. Nat Biotechnol 37:1372–1379

20. Fischer IH, Rezende JAM (2008) Diseases of passion flower (*Passiflora* spp). Pest Technol 2:1–19
21. Giraldo-González JJ, Carvalho FMS, Ferro JA, Herai RH, Chaves Bedoya G, Rodas Mendoza EF (2021) Transcriptional changes involved in kumquat (*Fortunella* spp) defense response to *Xanthomonas citri* subsp. *citri* in early stages of infection. Physiol Mol Plant Pathol 116:101729
22. Grabherr MG, Haas BJ, Yassour M, Levin JZ, Thompson DA, Amit I et al (2011) Full-length transcriptome assembly from RNA-Seq data without a reference genome. Nat Biotechnol 29:644–652
23. Gupta PK (2020) SWEET genes for disease resistance in plants. Trends Genet 36:901–904
24. Gupta PK, Balyan HS, Gautam T (2021) SWEET genes and TAL effectors for disease resistance in plants: present status and future prospects. Mol Plant Pathol 22:1014–1026
25. Haas BJ, Papanicolaou A, Yassour M, Grabherr M, Blood PD, Bowden J et al (2013) *De novo* transcript sequence reconstruction from RNA-seq using the Trinity platform for reference generation and analysis. Nat Protoc 8:1494–1512
26. Hu Y, Zhang J, Jia H, Sosso D, Li T, Frommer WB et al (2014) Lateral organ boundaries 1 is a disease susceptibility gene for citrus bacterial canker disease. PNAS 111:E521–E529
27. Huerta-Cepas J, Forslund K, Coelho LP, Szklarczyk D, Jensen LJ, von Mering C et al (2017) Fast genome-wide functional annotation through orthology assignment by eggNOG-Mapper. Mol Biol Evol 34:2115–2122
28. Ishida AKN, Halfeld-Vieira BA (2009) Mancha-bacteriana do maracujazeiro (*Xanthomonas axonopodis* pv. *passiflorae*): etiologia e estratégias de controle. In Documentos 357, Embrapa Amazônia Oriental, Belém, pp. 1–25
29. Jiang S, Balan B, Assis RAB, Sagawa CHD, Wan X, Han S et al (2020) Genome-wide profiling and phylogenetic analysis of the SWEET sugar transporter gene family in walnut and their lack of responsiveness to Xanthomonas arboricola pv. juglandis infection. Int J Mol Sci 21:1251
30. Kadota Y, Sklenar J, Derbyshire P, Stransfeld L, Asai S, Ntoukakis V et al (2014) Direct regulation of the NADPH oxidase RBOHD by the PRR-associated kinase BIK1 during plant immunity. Mol Cell 54:43–55
31. Klopfenstein DV, Zhang L, Pedersen BS, Ramírez F, Vesztrocy AW, Naldi A et al (2018) GOATOOLS: a python library for gene ontology analyses. Sci Rep 8:10872
32. Li Q, Qi J, Qin X, Hu A, Fu Y, Chen S et al (2021) Systematic identification of lysin-motif receptor-like kinases (LYKs) in *Citrus sinensis*, and analysis of their inducible involvements in citrus bacterial canker and phytohormone signaling. Sci Hortic 276:109755
33. Liu B, Li JF, Ao Y, Qu J, Li Z, Su J et al (2012) Lysin motif–containing proteins LYP4 and LYP6 play dual roles in peptidoglycan and chitin perception in rice innate immunity. Plant Cell 24:3406–3419
34. Livak KJ, Schmittgen TD (2001) Analysis of relative gene expression data using real-time quantitative PCR and the $2^{-\Delta\Delta CT}$ method. Methods 25:402–408
35. Lopes R, Lopes MTG, Carneiro MS, Matta FDP, Camargo LEA, Vieira MLC (2006) Linkage and mapping of resistance genes to *Xanthomonas axonopodis* pv. *passiflorae* in yellow passion fruit. Genome 49:17–29
36. Love MI, Huber W, Anders S (2014) Moderated estimation of fold change and dispersion for RNA-seq data with DESeq2. Genome Biol 15:1–21
37. Lu S, Wang J, Chitsaz F, Derbyshire MK, Geer RC, Gonzales NR et al (2020) CDD/SPARCLE: the conserved domain database in 2020. Nucleic Acids Res 48:D265–D268
38. MacManes MD (2018) The Oyster River Protocol: a multi-assembler and kmer approach for *de novo* transcriptome assembly. PeerJ. 2018:e5428
39. Manni M, Berkeley MR, Seppey M, Simão FA, Zdobnov EM (2021) BUSCO update: novel and streamlined workflows along with broader and deeper phylogenetic coverage for scoring of eukaryotic, prokaryotic, and viral genomes. Mol Biol Evol 38:4647–4654

40. Munhoz CF, Weiss B, Hanai LR, Zucchi MI, Fungaro MHP, Oliveira ALM et al (2011) Genetic diversity and a PCR-based method for *Xanthomonas axonopodis* detection in passion fruit. Phytopathology 101:416–424
41. Munhoz CF, Santos AA, Arenhart RA, Santini L, Monteiro-Vitorello CB, Vieira MLC (2015) Analysis of plant gene expression during passion fruit- *Xanthomonas axonopodis* interaction implicates lipoxygenase 2 in host defence. Ann Appl Biol 167:135–155
42. Nakayinga R, Makumi A, Tumuhaise V, Tinzaara W (2021) *Xanthomonas* bacteriophages: a review of their biology and biocontrol applications in agriculture. BMC Microbiol 21:1–20
43. Omasits U, Ahrens CH, Müller S, Wollscheid B (2014) Protter: interactive protein feature visualization and integration with experimental proteomic data. Bioinformatics 30:884–886
44. Peng A, Chen S, Lei T, Xu L, He Y, Wu L et al (2017) Engineering canker-resistant plants through CRISPR/Cas9-targeted editing of the susceptibility gene CsLOB1 promoter in citrus. Plant Biotechnol J 15:1509–1519
45. Pereira GS, Laperuta LDC, Nunes ES, Chavarría L, Pastina MM, Gazaffi R et al (2017) The sweet passion fruit (*Passiflora alata*) crop: genetic and phenotypic parameter estimates and QTL mapping for fruit traits. Trop. Plant Biol 10:18–29
46. Pruitt RN, Schwessinger B, Joe A, Thomas N, Liu F, Albert M et al (2015) The rice immune receptor XA21 recognizes a tyrosine-sulfated protein from a Gram-negative bacterium. Sci Adv 1(6):e1500245
47. Rutledge RG, Côté C (2003) Mathematics of quantitative kinetic PCR and the application of standard curves. Nucleic Acids Res 31(16):e93
48. Schmieder R, Edwards R (2011) Quality control and preprocessing of metagenomic datasets. Bioinformatics 27:863–864
49. Sheikh-Assadi M, Naderi R, Salami SA, Kafi M, Fatahi R, Shariati V et al (2022) Normalized workflow to optimize hybrid *de novo* transcriptome assembly for non-model species: a case study in *Lilium ledebourii* (Baker) Boiss. Plants 11(18):2365
50. Slewinski TL (2011) Diverse functional roles of monosaccharide transporters and their homologs in vascular plants: a physiological perspective. Mol Plant 4:641–662
51. Smith-Unna R, Boursnell C, Patro R, Hibberd JM, Kelly S (2016) TransRate: reference-free quality assessment of de novo transcriptome assemblies. Genome Res 26(8):1134–1144
52. Teper D, Wang N (2021) Consequences of adaptation of TAL effectors on host susceptibility to *Xanthomonas*. PLoS Genet 17:e1009310
53. Teper D, Xu J, Li J, Wang N (2020) The immunity of meiwa kumquat against *Xanthomonas citri* is associated with a known susceptibility gene induced by a transcription activator-like effector. PLOS Pathog 16:e1008886
54. Timilsina S, Potnis N, Newberry EA, Liyanapathiranage P, Iruegas-Bocardo F, White FF et al (2020) *Xanthomonas* diversity, virulence and plant–pathogen interactions. Nat Rev Microbiol 18:415–427
55. Toruño TY, Stergiopoulos I, Coaker G (2016) Plant-pathogen effectors: cellular probes interfering with plant defenses in spatial and temporal manners. Annu Rev Phytopathol 54:419–441
56. Tripathi L, Tripathi JN, Shah T, Muiruri KS, Katari M (2019) Molecular basis of disease resistance in banana progenitor *Musa balbisiana* against *Xanthomonas campestris* pv. *musacearum*. Sci. Rep. 9:1–17
57. Xia Z, Huang D, Zhang S, Wang W, Ma F, Wu B et al (2021) Chromosome-scale genome assembly provides insights into the evolution and flavor synthesis of passion fruit (*Passiflora edulis* Sims). Hortic Res 8:14
58. Xu C, Luo F, Hochholdinger F (2016) LOB domain proteins: beyond lateral organ boundaries. Trends Plant Sci 21:159–167
59. Xuan YH, Hu YB, Chen LQ, Sosso D, Ducat DC, Hou BH et al (2013) Functional role of oligomerization for bacterial and plant SWEET sugar transporter family. PNAS 110:E3685–E3694

60. Yu Y, Zhang G, Chen Y, Bai Q, Gao C, Zeng L et al (2019) Selection of reference genes for qPCR analyses of gene expression in ramie leaves and roots across eleven abiotic/biotic treatments. Sci Rep 9:1–13

Figures

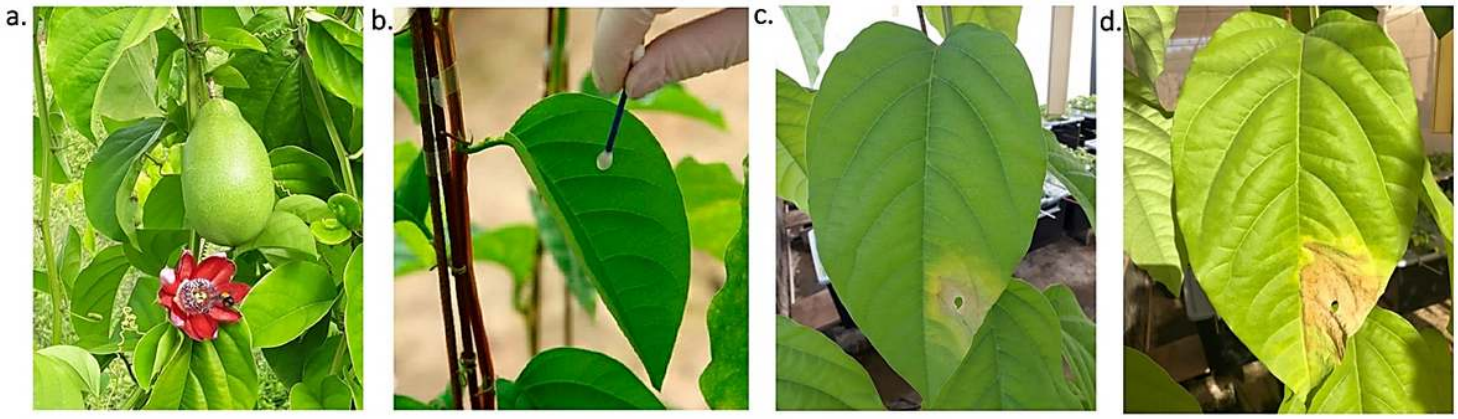

Figure 1

A sweet passion fruit (*Passiflora alata*) specimen under field conditions (a). (Photo credit: A. R. Benedetti, Escola Superior de Agricultura "Luiz de Queiroz", Universidade de São Paulo, Brazil). In sequence, leaf inoculation with *Xanthomonas axonopodis* (b) and progression of lesions after 20 (c) and 30 (d) days after inoculation.

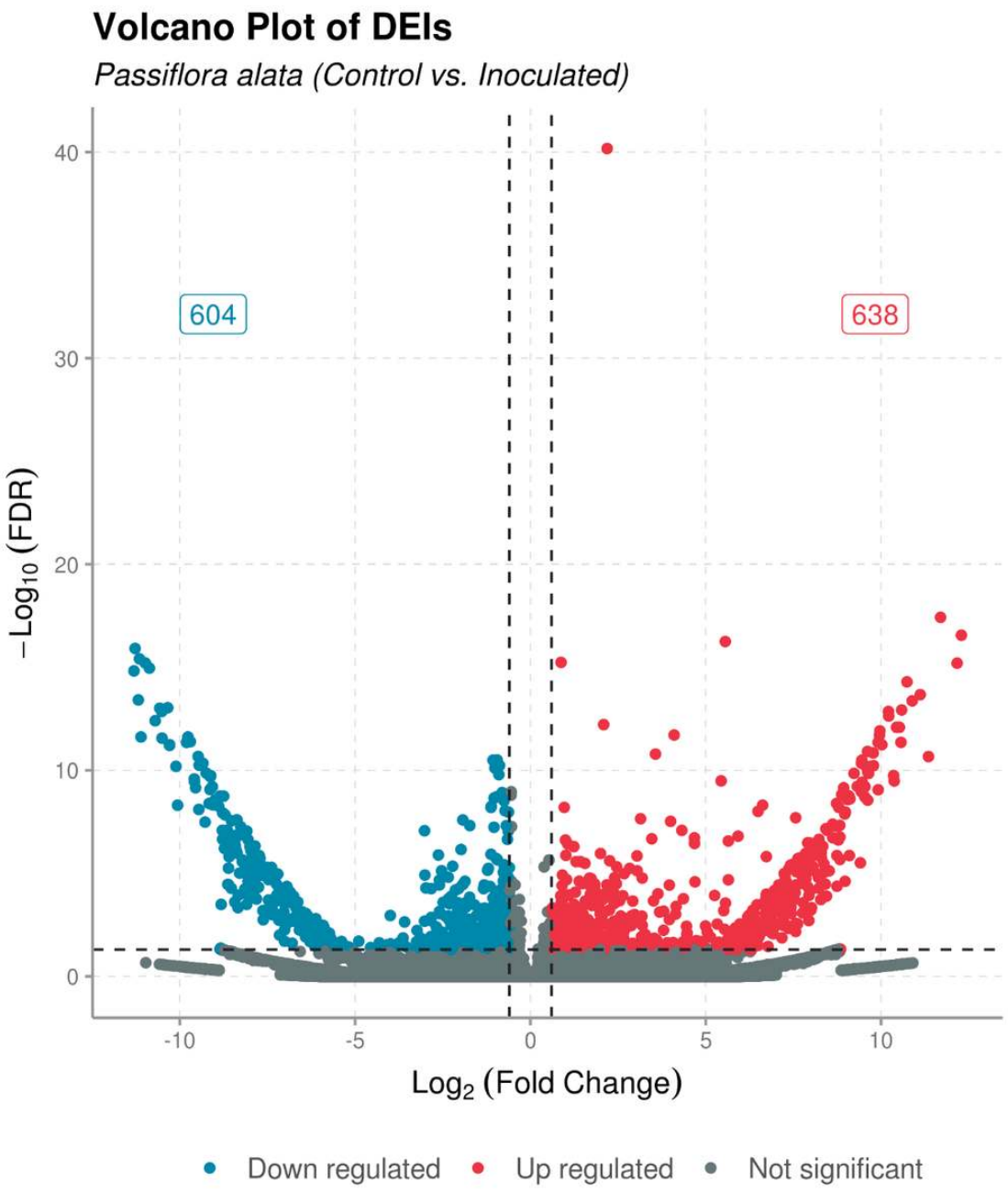

Figure 2

Visualization of RNA-seq results (Volcano plot). The Log_2 (fold change) indicates the mean expression level for each gene, and blue and red dots represent downregulated and upregulated genes, respectively, in the inoculated group compared to the mock-inoculated (control) group. Grey dots indicate the transcripts with no difference in expression between the two groups.

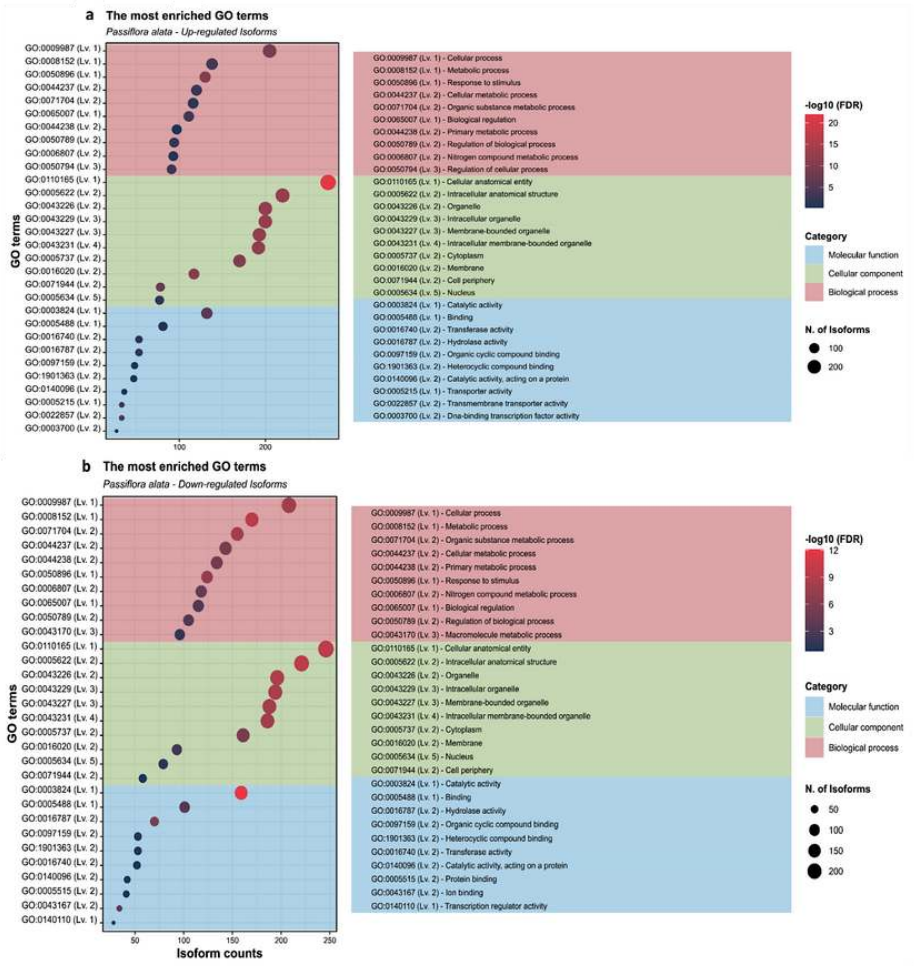

Figure 3

Bubble plot displaying GO pathway enrichment analysis using the top 10 GO terms. The up- (a) and downregulated (b) transcripts were classified into three categories shown in the pink (Molecular function), green (Cellular component) and blue (Biological process) rectangles. Only significantly enriched terms with p values < 0.05 are specified. The colors of each bubble represent the values of $-\mathrm{Log}_{10}$ (FDR). The higher the $-\mathrm{Log}_{10}$ (FDR) value, the higher the statistical significance. On each pathway, bubble sizes are proportional to the number of differentially expressed transcripts.

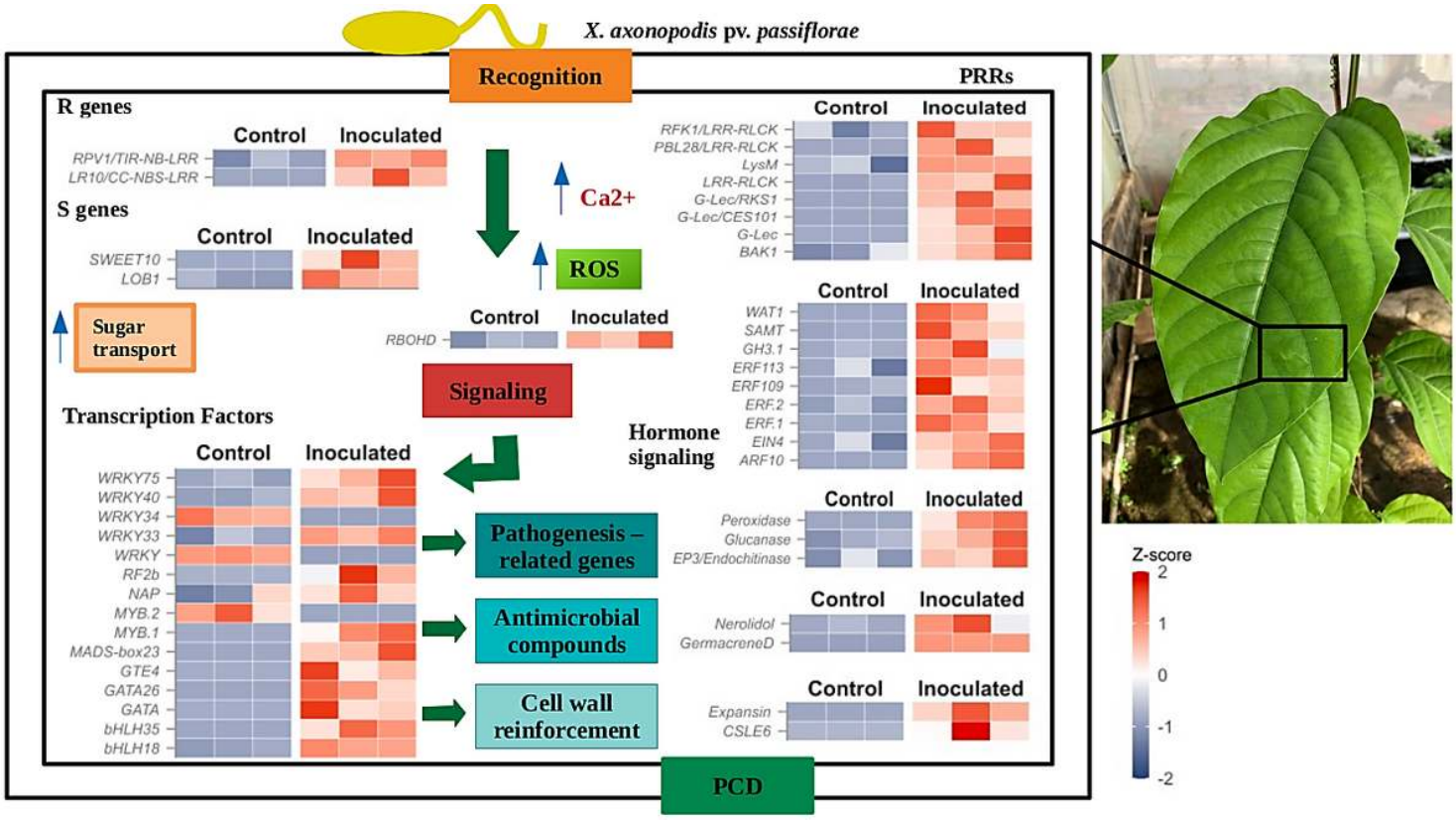

Figure 4

Expression profiling of *Passiflora alata* in response to *Xanthomonas axonopodis*. Once the pathogen was recognized by PRRs or *R* genes, there was an increase in calcium influx and ROS accumulation, triggering a signaling cascade, leading to activation of hormone-related genes and transcription factors that act to regulate genes associated with pathogenesis, antimicrobial compounds and cell wall expansion. Blue rectangles represent the three biological replicates obtained from mock-inoculated samples and orange rectangles represent the three biological replicates obtained from inoculated samples.

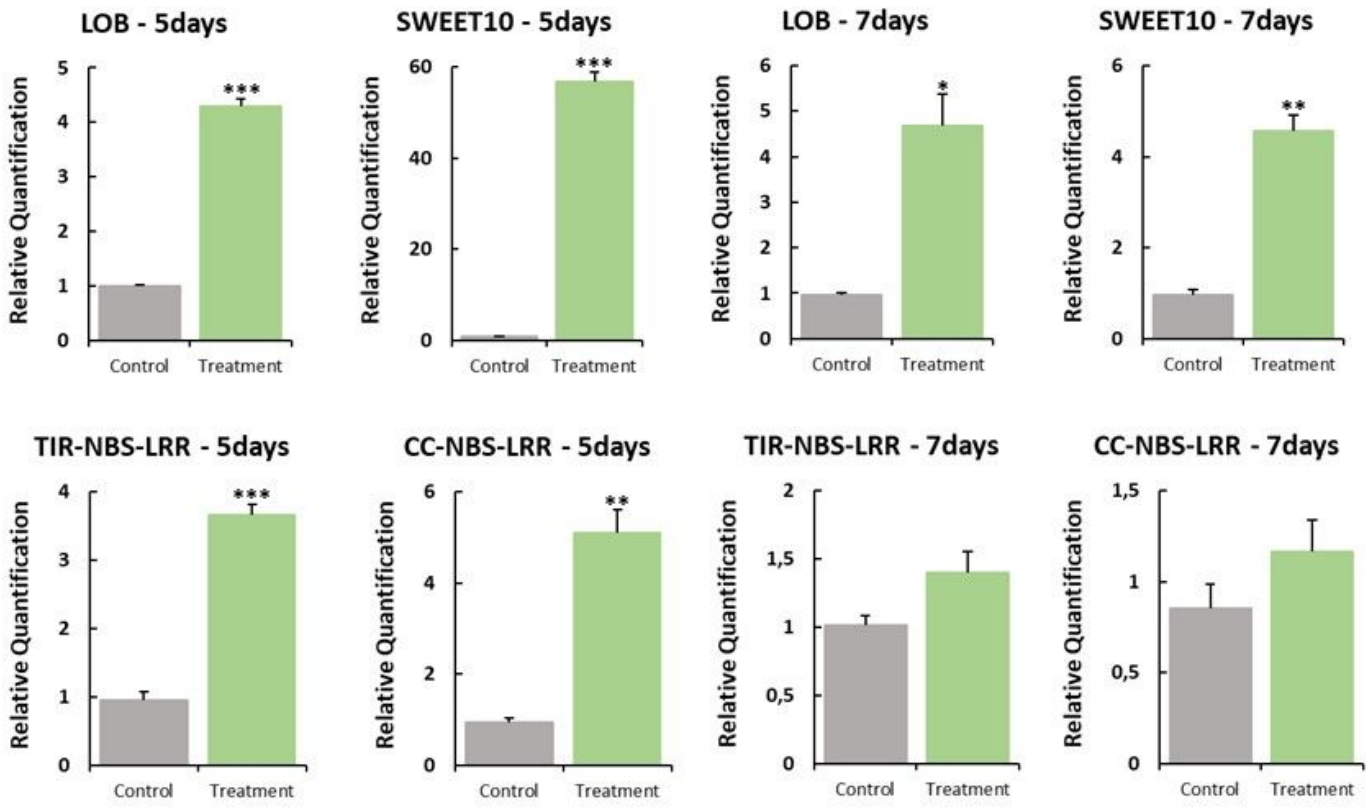

Figure 5

Quantitative real-time PCR results. The expression levels of 2 susceptibility genes (*LOB* and *SWEET10*) and 2 resistance genes (*TIR-NBS-LRR* and *CC-NBS-LRR*) were evaluated at 5 DAI and 7 DAI. At an earlier stage, all showed statistically significant differences in expression level and were upregulated in leaves inoculated with*Xanthomonas axonopodis* pv. *passiflorae* compared to the controls. Note that both resistance genes decreased their expression levels at a later stage (7 DAI), showing no statistically significant differences compared to the controls.

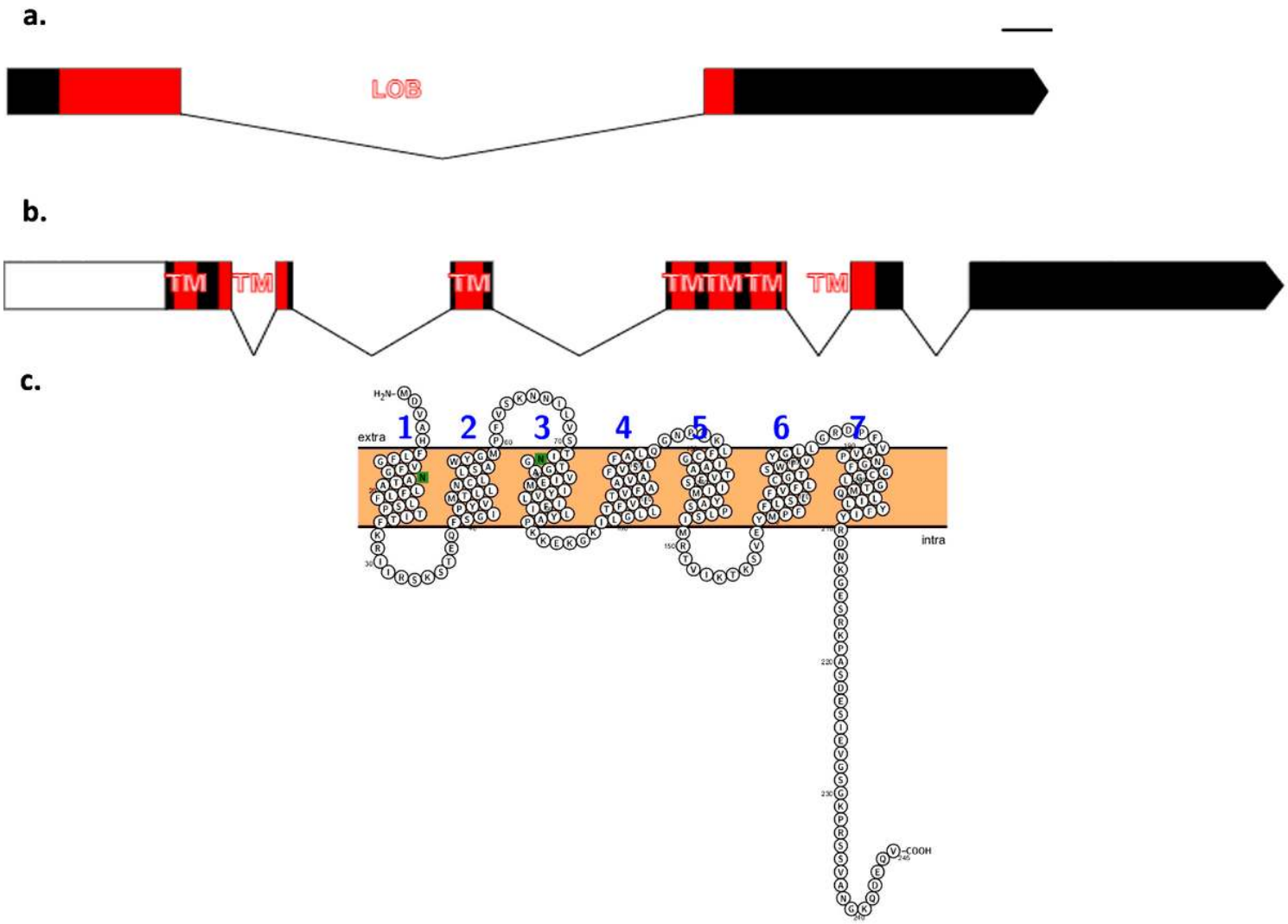

Figure 6

Structure of *Passiflora LOB1* and *SWEET10* gene. Intron-exon boundary of *LOB1* gene (evm.model.scaffold10_size6807042.313). Black boxes represent the coding region. LOB (in red) is the main domain; bar 100 bp (a). Intron-exon boundary of *SWEET10* (evm.model.scaffold23_size2064600.16). The white box represents the 5' UTR and black boxes represent the coding region. TMs (in red) are transmembrane domains (b). Predicted protein sequence and transmembrane topology of *SWEET10*. N denotes glycosylated residues (c).

Supplementary Files

This is a list of supplementary files associated with this preprint. Click to download.

- CardosoetalSupplementaryMaterial2523.docx
- SupplementaryFile01280223.xlsx